J. Phys. B: At. Mol. Opt. Phys. **44** (2011) 085201 (6pp) doi:10.1088/0953-4075/44/8/085201

Calibration of distorted wave Born approximation for electron impact excitation of Ne and Ar at incident energies below 100 eV

Yaqiu Liang[1], Zhangjin Chen[2], D H Madison[3] and C D Lin[2]

[1] College of Physics, Liaoning University, Shenyang 110036, People's Republic of China
[2] J R Macdonald Laboratory, Physics Department, Kansas State University, Manhattan, KS 66506-2604, USA
[3] Physics Department, Missouri University of Science and Technology, Rolla, MO 65401, USA

E-mail: zjchen@phys.ksu.edu

Received 21 January 2011, in final form 10 March 2011
Published 11 April 2011
Online at stacks.iop.org/JPhysB/44/085201

Abstract
We calibrate the distorted wave Born approximation (DWBA) for electron impact excitation processes empirically. Differential cross sections (DCSs) for the excitation of the $2p^5 3s$, $2p^5 3p$, $2p^5 4s$ and $2p^5 4p$ configurations of Ne and the $3p^5 4s$ and $3p^5 4p$ configurations of Ar by electron impact are calculated using DWBA for incident energies between 20 and 100 eV. The calculated results are compared with the absolute experimental measurements and other theoretical results. We found that the structure of the DCS can be well reproduced by the DWBA model while the magnitude is overestimated for most cases considered here. The differences in magnitude between DWBA and experiment are used to test the calibration of DWBA such that the DWBA can be used to describe laser-induced electron impact excitation processes. These processes are involved in the non-sequential double ionization of atoms in strong laser fields.

(Some figures in this article are in colour only in the electronic version)

1. Introduction

The process of nonsequential double ionization (NSDI) of atoms in linearly polarized laser pulses is one of the most interesting and challenging topics in strong field physics. In NSDI, one electron that is first released near the maximum of the oscillating electric field may be driven back to revisit the parent ion when the electric field is near zero. When the returning electron collides with the parent ion with energies above the ionization threshold, it may kick out another bound electron, resulting in an (e, 2e)-like process. The returning electron may also excite the bound electron to a higher excited state which is subsequently tunnel ionized when the electric field increases again. Since 2000, complete experimental measurements on the full momentum vectors of the two outgoing electrons along the direction of polarization of the laser pulse have become available [1, 2], and a number of theoretical studies have also been carried out.

Recently, Chen *et al* [3] have developed a quantitative rescattering (QRS) theory which has been applied to various rescattering processes induced by short intense laser pulses [4–9]. The significant advantage of the QRS theory is that it treats rescattering processes in the laser field as laser-*free* scattering processes, where the laser-induced returning electrons are described by a wavepacket. The QRS enables us to simulate two-dimensional correlated momentum distributions for NSDI *quantitatively* and the necessary input data are the triple differential cross sections (TDCS) for (e, 2e) [8] and the differential cross sections (DCS) for electron impact excitation of ions [9]. However, to obtain the correlated momentum spectra that can be compared with experimental measurements, one needs to have the TDCS for (e, 2e)

ionization and the DCS for excitation for all possible momenta of the returning electrons. For NSDI of atoms in strong laser pulses, the highest energy, $E_i^{\max}$, of the returning (incident) electron is determined by the laser field, which is less than 100 eV for typical 800 nm lasers. Consequently to simulate the correlated momentum distributions for NSDI, accurate DCSs for electron impact excitation of the parent ion for all incident energies from threshold to $E_i^{\max}$ and all possible excited states are needed. Therefore, we require a theoretical approach which can provide these quantities quickly and accurately.

Numerous theoretical methods have been used for calculating electron-impact excitation DCSs, including distorted wave Born approximation (DWBA) [10], second-order distorted wave model [11], *R*-matrix method [12] and convergent close-coupling (CCC) calculations [13]. The sophisticated theoretical models, such as CCC and the *R*-matrix method, are capable of predicting accurate angular DCS, as well as the absolute magnitude. For higher energies, both the integrated and DCS predicted by DWBA are fairly accurate. To perform QRS calculations, it would be best to use the R-matrix or CCC approach for low energies, and the DWBA for high energies. However, there is such a large number of cross sections needed for the QRS calculations that it is not practical to use numerically intensive approaches such as the *R*-matrix or CCC to generate the required data.

While the DWBA is ideally suited for these calculations since it can be calculated very quickly, it is well known that, at low energies, the total cross sections (TCS) predicted by the DWBA significantly exceed the experimental values and that the DWBA DCS are also larger than absolute experimental data. However, the shape of the DWBA DCS is typically in fairly good agreement with the experimental measurements. Only recently absolute measurements have been made for TDCS for (e, 2e) scattering and it was also found that the DWBA agreed very nicely with the shape but not the absolute value [14]. This suggests that the DWBA contains the important physics which determines the shape of angular distributions correctly but not the absolute value which is just an overall normalization constant. Consequently one could use the DWBA for low energies if there was a way to renormalize the absolute value. Here we present a renormalization procedure based upon absolute experimental DCS data.

The organization of this paper is as follows: in section 2, the basic theory of DWBA for electron impact excitation is presented. In section 3, the DWBA DCS for electron impact excitation of Ne and Ar at incident energies below 100 eV are compared with the absolute experimental data and it is shown that relatively good agreement with experiment can be achieved with proper renormalization. In section 4, a calibration procedure is proposed using the TCS.

Atomic units are used in this paper unless otherwise specified.

2. Theory

In this section, we present the DWBA theory for electron impact excitation of atoms. The formulas presented here are generic and therefore can easily be applied to the processes of electron impact excitation of ions which are involved in NSDI.

Suppose we have an electron with momentum $\mathbf{k}_i$ which collides with an atom A, after the collision, the scattered electron has momentum $\mathbf{k}_f$, and one bound electron in atom A is excited to a higher energy bound state. In the frozen core approximation, the 'exact' Hamiltonian for the whole system is

$$H = -\frac{1}{2}\nabla_1^2 + V_{A^+}(r_1) - \frac{1}{2}\nabla_2^2 + V_{A^+}(r_2) + \frac{1}{r_{12}}, \qquad (1)$$

where $\mathbf{r}_1$ and $\mathbf{r}_2$ are the position vectors for the projectile and the bound state electron with respect to the nucleus, respectively. This Hamiltonian can be rewritten approximately as

$$H_j = -\tfrac{1}{2}\nabla_1^2 + U_j(r_1) - \tfrac{1}{2}\nabla_2^2 + V_{A^+}(r_2) \quad (j = i, f). \qquad (2)$$

In this equation, U_i (U_f) is the distorting potential used to calculate the initial (final) state wavefunction $\chi_{\mathbf{k}_i}$ ($\chi_{\mathbf{k}_f}$) for the projectile. In the DWBA, the direct transition amplitude for excitation from an initial state Ψ_i to a final state Ψ_f is expressed by

$$f = \langle \chi^-_{\mathbf{k}_f}(1)\Psi_f(2)|V_i|\Psi_i(2)\chi^+_{\mathbf{k}_i}(1)\rangle, \qquad (3)$$

where V_i is the perturbation interaction:

$$V_i = H - H_i = \frac{1}{r_{12}} + V_{A^+}(r_1) - U_i(r_1). \qquad (4)$$

In equation (3), the initial and final state wavefunctions for the projectile satisfy the differential equation

$$\left[-\tfrac{1}{2}\nabla_1^2 + U_j(r_1) - \tfrac{1}{2}k_j^2\right]\chi_{\mathbf{k}_j}(\mathbf{r}_1) = 0 \quad (j = i, f), \qquad (5)$$

and the bound state wavefunctions are the eigenfunctions of the equation

$$\left[-\tfrac{1}{2}\nabla_2^2 + V_{A^+}(r_2) - \epsilon_j\right]\Psi_j(\mathbf{r}_2) = 0 \quad (j = i, f), \qquad (6)$$

where ϵ_j ($j = i, f$) are the corresponding eigenenergies of the initial and final bound states which can be expressed as

$$\Psi_j(\mathbf{r}) = \psi_{N_jL_j}(r)Y_{L_jM_j}(\hat{\mathbf{r}}) \quad (j = i, f). \qquad (7)$$

The exchange scattering amplitude is given by

$$g = \langle \Psi_f(1)\chi^-_{\mathbf{k}_f}(2)|V_i|\Psi_i(2)\chi^+_{\mathbf{k}_i}(1)\rangle. \qquad (8)$$

Finally, the differential cross section for electron impact excitation is given by

$$\frac{\mathrm{d}\sigma}{\mathrm{d}\Omega} = N(2\pi)^4\frac{k_f}{k_i}\frac{1}{2L_i+1} \times \sum_{M_i=-L_i}^{+L_i}\sum_{M_f=-L_f}^{+L_f}\left(\frac{3}{4}|f-g|^2 + \frac{1}{4}|f+g|^2\right). \qquad (9)$$

The prefactor N in equation (9) denotes the number of electrons in the subshell from which one electron is excited.

The distorting potentials, U_i and U_f, used in equation (5) to calculate the wavefunctions for the projectile in the initial

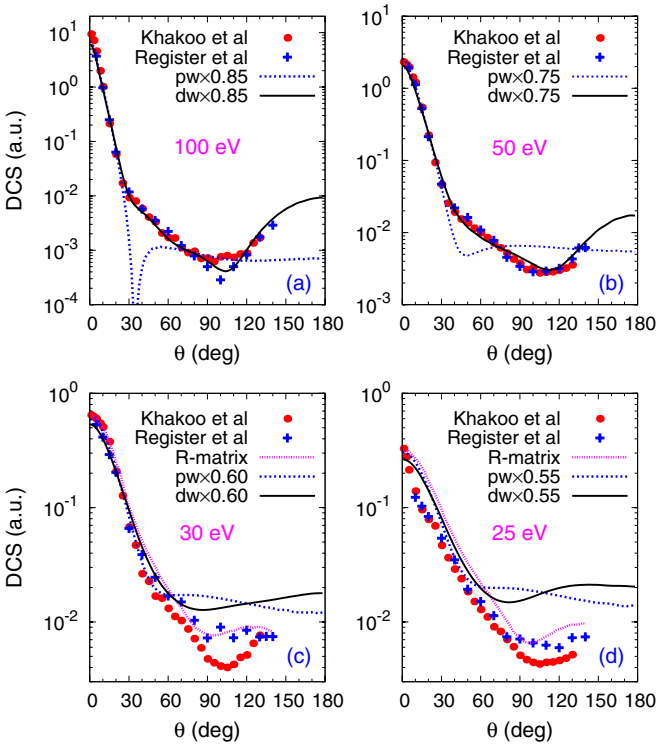

Figure 1. DCS for the excitation of the $2p^5 3s$ configuration of Ne by electron impact at incident energies of (a) 100 eV, (b) 50 eV, (c) 30 eV and (d) 25 eV. The absolute experimental measurements are from Register *et al* [16] and Khakoo *et al* [17]. For incident energies of 30 and 25 eV, the *R*-matrix results of Khakoo *et al* [17] are also plotted for comparison.

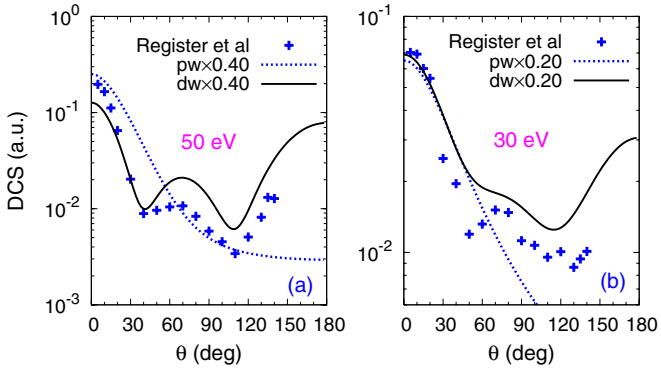

Figure 2. The same as figure 1 but for the $2p^5 3p$ configuration at incident energies of (a) 50 and (b) 30 eV.

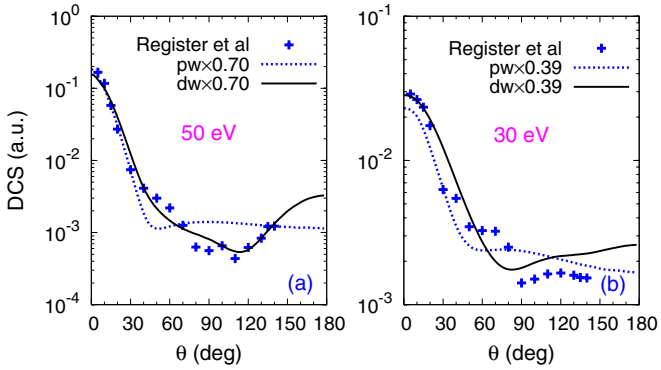

Figure 3. The same as figure 1 but for the $2p^5 4s$ configuration at incident energies of (a) 50 and (b) 30 eV.

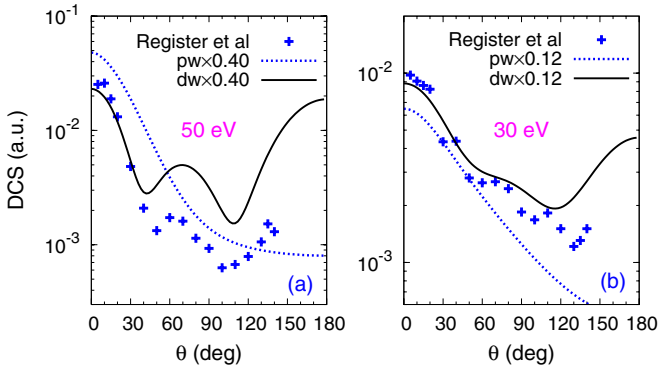

Figure 4. The same as figure 1 but for the $2p^5 4p$ configuration at incident energies of (a) 50 and (b) 30 eV.

and final states, respectively, are not determined directly by the formalism. Here, we use static potentials which take the form as

$$U_j(r_1) = V_{A^+}(r_1) + \int \mathrm{d}\mathbf{r}_2 \frac{|\Psi_j(\mathbf{r}_2)|^2}{r_{12}} \quad (j = i, f). \quad (10)$$

As shown previously, $V_{A^+}(r)$ in equation (10) is the atomic potential used to evaluate eigenstate wavefunctions of the bound state electron. Here we use the effective potential from Tong and Lin [15] based on single active electron approximation, which is given by

$$V_{A^+}(r) = -\frac{1 + a_1 e^{-a_2 r} + a_3 r e^{-a_4 r} + a_5 e^{-a_6 r}}{r}, \quad (11)$$

where the parameters a_i, as given explicitly in table 1 in [15], are obtained by fitting the calculated binding energies from this potential to the experimental ones of the ground state and the first few excited states of the target atom.

3. Results and discussions

The perturbative nature of the DWBA causes it to overestimate electron impact excitation cross sections of ions at low energies. To calibrate the DWBA theory, one should compare its predictions to accurate theoretical results or absolute experimental measurements. Unfortunately, neither are easily available for atomic and molecular ions. Thus we use neutral Ne and Ar atoms for the calibration.

In figures 1–4, the DWBA DCSs for the excitation of the $2p^5 3s$, $2p^5 3p$, $2p^5 4s$ and $2p^5 4p$ configurations of Ne for incident energies of 100 eV and below are compared with the absolute experimental data [16, 17]. For the $2p^5 3s$ configuration, the DCSs from the *R*-matrix theory are also plotted for incident energies of 30 and 25 eV. It can be seen from figures 1–4 that the DWBA overestimates the DCSs for all the cases considered here. To get the best overall agreement, different normalization factors are assigned to the DWBA for different configurations and different incident energies. For

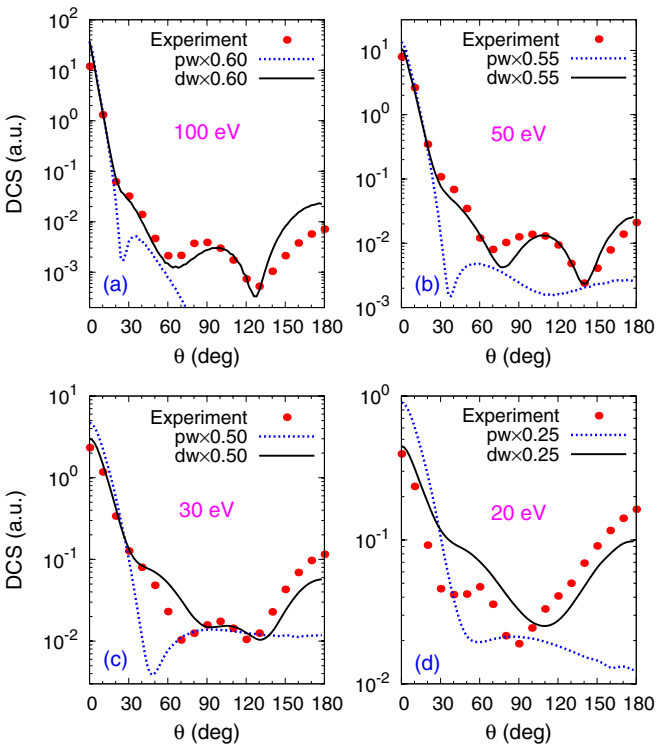

Figure 5. DCS for the excitation of the $3p^5 4s$ configuration of Ar by electron impact at incident energies of (a) 100 eV, (b) 50 eV, (c) 30 eV and (d) 20 eV. The absolute experimental measurements are from Chutjian and Cartwright [18].

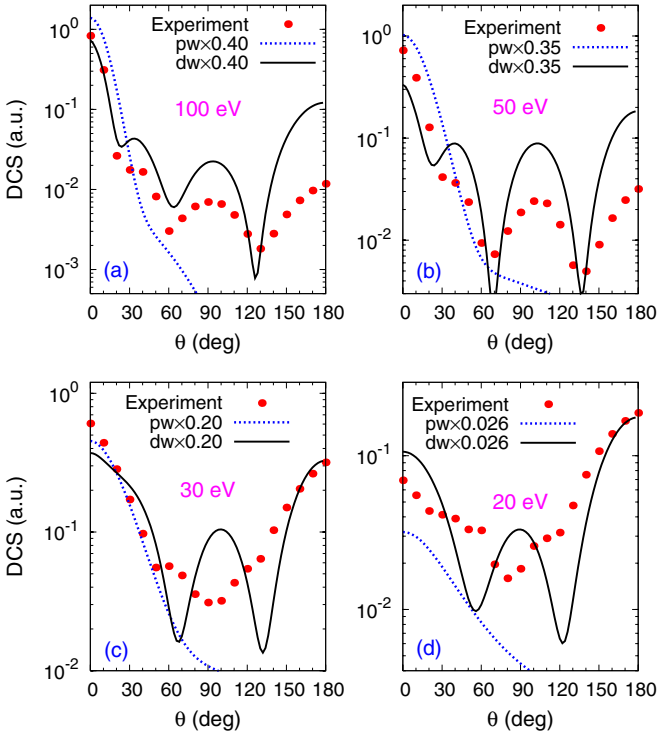

Figure 6. The same as figure 5 but for the $3p^5 4p$ configuration at incident energies of (a) 100, (b) 50, (c) 30 and (d) 20 eV.

incident energies below 30 eV, the DCSs of the DWBA are 2–7 times higher than the experimental measurements. However, it is seen that reasonably good agreement with experiment is achieved for almost all cases after renormalization. The worst agreement is found for the larger scattering angles where the cross section is smaller by one or more orders of magnitude.

To see the distorting effect from the DWBA, the results of the plane wave Born approximation (PWBA), in which plane waves are used to describe the projectile electron in both the initial and final states, are also displayed for comparison. For scattering angles greater than 30°, one can see that the PWBA fails completely in predicting the angular distributions even for incident energy of 100 eV. In contrast, the enhanced DCSs for backward scattering observed in experiment are reasonably well reproduced by the DWBA.

In figures 5 and 6, we show similar comparison for the excitation of $3p^5 4s$ and $3p^5 4p$ configurations of Ar. The experimental measurements were performed by Chutjian and Cartwright [18]. Compared to the excitation of Ne, the DCS of Ar have more structure. For example, for $3p^5 4s$ at 100 and 50 eV, as shown in figures 5(a) and (b), in addition to the rapid slope change around 25°, extra minima were observed in experiment which are reproduced by the DWBA. For $3p^5 4p$ at 100 and 50 eV, as shown in figures 6(a) and (b), the DWBA predicts a triple minima in the DCS. That was observed in experiment as well. Although the backscattering is overestimated by the DWBA, these cross sections are fairly small. This might indicate that the distorting potential used in the calculations needs to be improved. For lower incident energies of 30 and 20 eV, the agreement between DWBA and experiment for $3p^5 4p$ of Ar cannot be regarded as satisfactory. However, the main features are still predicted by the DWBA.

4. Calibration of the DWBA

In the last section it was shown that, for the most part, reasonably good agreement between absolute experimental DCS and the DWBA could be achieved by renormalizing the DWBA. The worst agreement was found for the smallest cross sections and even here the DWBA properly predicted the measured structure. The renormalized DWBA results would be fine for use in a QRS calculation. To use the DWBA in a QRS calculation, we need a calibration procedure for any energy between threshold and 100 eV that is quick and accurate. We turn to the TCS for this calibration procedure.

Tong *et al* [19] proposed an empirical method to evaluate the TCS for electron impact excitation:

$$\sigma_{\mathrm{Tong}}(E_i) = \alpha \frac{\pi}{\Delta E^2} e^{1.5(\Delta E - \epsilon)/E_i} f\left(\frac{E_i}{\Delta E}\right), \qquad (12)$$

where

$$f(x) = \frac{1}{x}\left[\beta \ln x - \gamma\left(1 - \frac{1}{x}\right) + \delta \frac{\ln x}{x}\right]. \qquad (13)$$

In equation (12), ΔE is the excitation energy for a given transition, and ϵ is the eigenenergy of the corresponding

excited state. The parameters in equation (13) have been obtained initially by fitting to the CCC excitation cross sections for hydrogen and He^+. Explicitly, these parameters are $\beta = 0.7638$, $\gamma = 1.1759$ and $\delta = 0.6706$.

The original formula given by Tong *et al* does not have the prefactor α which is added in this work to ensure that the empirical formula reproduces the same cross sections for each excited state as those from the DWBA at high energies since the DWBA is known to be accurate for high energies. We have normalized the Tong *et al* TCS to the DWBA TCS at an energy of 500 eV for each excited state.

The TCS of the DWBA at a fixed incident energy $E_i = k_i^2/2$ can be obtained by integrating the DCS of equation (9) over scattering angles:

$$\sigma_{\mathrm{DWBA}}(E_i) = \int \frac{\mathrm{d}\sigma}{\mathrm{d}\Omega} d\hat{\mathbf{k}}_f. \tag{14}$$

Since the normalized DWBA is in reasonably good agreement with absolute experimental data, the integral of the normalized DWBA DCS, say $\mathcal{C}(E_i)\sigma_{\mathrm{DWBA}}(E_i)$, where $\mathcal{C}(E_i)$ is the normalization constant for a particular state and energy, represents an approximation for the absolute experimental TCS. If σ_{Tong} were an accurate TCS, it should be the same, i.e.

$$\sigma_{\mathrm{Tong}}(E_i) = \mathcal{C}(E_i)\sigma_{\mathrm{DWBA}}(E_i). \tag{15}$$

Consequently, if σ_{Tong} was accurate, the ratio

$$\mathcal{C}(E_i) = \sigma_{\mathrm{Tong}}(E_i)/\sigma_{\mathrm{DWBA}}(E_i) \tag{16}$$

would be the same as the normalization factors found in figures 1–6. If this is the case, then the scaling factor in equation (16) could be used to normalize the DCS of DWBA at different incident energies.

The empirical formula, equation (12), has already been used to calculate the total ionization yield of Ar in NSDI as a function of the peak intensity for a linearly polarized laser pulse by Micheau *et al* [7].

To obtain the scaling factor $\mathcal{C}(E_i)$ for electron-Ne excitation, we calculate the TCSs using the DWBA and those using equation (12) for all the four configurations considered here at incident energies from threshold up to 500 eV. These TCSs for incident energies below 120 eV are shown in figure 7 referring to the left vertical axis. It can be seen that the difference in the magnitude of TCS between the DWBA and Tong *et al* increases with decreasing incident energy. The ratio of theoretical cross sections, i.e. the scaling factor $\mathcal{C}(E_i)$, is also plotted in figure 7, referring to the right vertical axis. The normalization factors used in figures 1–4 for DWBA to obtain the best overall agreement with the experimental DCSs are displayed for comparison. These normalization factors (solid circles) can be regarded as absolute experimental ratios so this is the equivalent of comparing experiment and theory. One can see that all the normalization factors used in figures 1–4 agree well with those predicted by the scaling factor $\mathcal{C}(E_i)$. In figure 8, similar comparisons for Ar are shown. The good agreement of $\mathcal{C}(E_i)$ with the normalization factors used in figures 5 and 6 confirms again the validity of the calibration method.

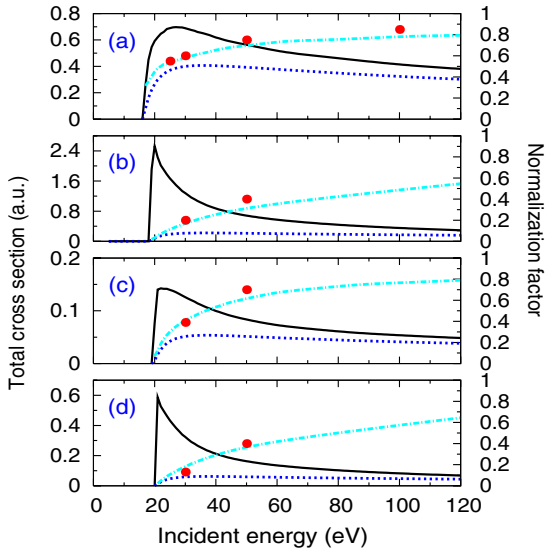

Figure 7. Total cross sections (left vertical axis) and normalization factors of DWBA (right vertical axis) for electron impact excitation of Ne from $2p^6$ to (a) $2p^5 3s$, (b) $2p^5 3p$, (c) $2p^5 4s$ and (d) $2p^5 4p$. Solid curve: total cross sections of DWBA; dotted curve: total cross sections calculated using the empirical formula of Tong *et al* [19]; chain curve: scaling factor $\mathcal{C}(E_i)$; solid circles: normalization factors used in figures 1–4 for DWBA to obtain the best overall agreement with experiment.

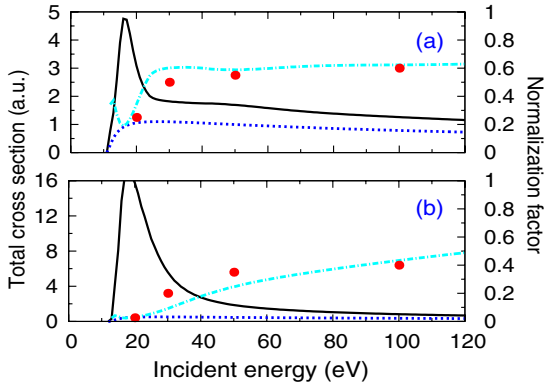

Figure 8. The same as figure 7 but for Ar from $3p^6$ to (a) $3p^5 4s$ and (b) $3p^5 4p$. The solid circles are the normalization factors used in figures 5 and 6 for DWBA to obtain the best overall agreement with experiment.

In conclusion, we proposed a method to calibrate the DCS from DWBA for electron impact excitation of atoms at low energies. The method will be applied to simulate the correlated electron momentum spectra for NSDI of atoms in a strong laser field, in which electron impact excitation of the parent ions is involved. This work paves the way for theoretical study, based on the QRS model, on NSDI of atoms in a strong laser pulse.

Acknowledgments

This work was supported in part by Chemical Sciences, Geosciences and Biosciences Division, Office of Basic Energy Sciences, Office of Science, US Department of Energy. YL was supported with financial aids from China Scholarship

Council, China Education Ministry under grant no 2009-1590, and Education Department in Liaoning Province of China under grant no 2009A305. The work of DHM was supported by the National Science Foundation under grant no PHY-0757749.

References

[1] Weber Th, Giessen H, Weckenbrock M, Urbasch G, Staudte A, Spielberger L, Jagutzki O, Mergel V, Vollmer M and Dörner R 2000 *Nature* **405** 658
[2] Staudte A *et al* 2007 *Phys. Rev. Lett.* **99** 263002
[3] Chen Z, Le A-T, Morishita T and Lin C D 2009 *Phys. Rev.* A **79** 033409
[4] Lin C D, Le A-T, Chen Z, Morishita T and Lucchese R 2009 *J. Phys. B: At. Mol. Opt. Phys.* **43** 122001
[5] Chen Z, Wittmann T, Horvath B and Lin C D 2009 *Phys. Rev.* A **80** 061402
[6] Liang Y 2010 *Phys. Rev.* A **82** 055403
[7] Micheau S, Chen Z, Le A-T and Lin C D 2009 *Phys. Rev.* A **79** 013417
[8] Chen Z, Liang Y and Lin C D 2010 *Phys. Rev. Lett.* **104** 253201
[9] Chen Z, Liang Y and Lin C D 2010 *Phys. Rev.* A **82** 063417
[10] Bartschat K and Madison D H 1987 *J. Phys. B: At. Mol. Phys.* **20** 5839
[11] Madison D H and Winters K H 1983 *J. Phys. B: At. Mol. Phys.* **16** 4437
[12] Zeman V and Bartschat K 1997 *J. Phys. B: At. Mol. Opt. Phys.* **30** 4609
[13] Bray I and Stelbovics Andris T 1992 *Phys. Rev.* A **46** 6995
[14] Ren X *et al* 2010 *Phys. Rev.* A **82** 032712
[15] Tong X M and Lin C D 2005 *J. Phys. B: At. Mol. Opt. Phys.* **38** 2593
[16] Register D F, Trajmar S, Steffensen G and Cartwright David C 1984 *Phys. Rev.* A **29** 1793
[17] Khakoo M A *et al* 2002 *Phys. Rev.* A **65** 062711
[18] Chutjian A and Cartwright D C 1981 *Phys. Rev.* A **23** 2178
[19] Tong X M, Zhao Z X and Lin C D 2003 *Phys. Rev.* A **68** 043412